COO 1721-81

OBSERVED SINGLE ATOM ELASTIC CROSS SECTIONS IN A SCANNING ELECTRON MICROSCOPE*†

M. Retsky††

Department of Physics, The University of Chicago
Chicago, Illinois 60637

ABSTRACT

Single atom elastic cross sections have been measured in a scanning electron microscope capable of resolving single atoms of $Z \geqslant 47$. These measurements have been made on Uranium, Mercury, and Silver at 50 kv. The measurements are in agreement with the best available calculations.

The major distinction between conventional measurements (using thin foils or gases) and the microscope measurement is the beam intensity. With Uranium, for example, during each measurement each Uranium atom experiences 4×10^5 elastic events and 9×10^4 inelastic events.

We have been able to experimentally distinguish single Silver atoms from Mercury or Uranium, but not Mercury atoms from Uranium. This is attributable to the 30% experimental standard deviation of the data. The sources of the standard deviation are discussed.

*Work supported by the U. S. Atomic Energy Commission.

†Submitted in partial fulfillment of the requirements for a Ph.D. from the Department of Physics, The University of Chicago

††Present address: Zenith Radio Corporation, Chicago, Illinois

DISCLAIMER

I. INTRODUCTION

Resolving and identifying single atoms is one of the most fundamental challenges in electron microscopy. Several recent reports [1-5] have been made claiming to have resolved single atoms in microscopes, but the atoms were identified primarily from the geometry of model compounds and scattering intensities have not been quantitatively related to the theoretical cross sections.

Cross section calculations for elastic electron collisions with single atoms have reached an advanced state, and they are referred to as "exact" in the literature.

This paper will not consider the various approximations to elastic scattering theory such as the Born approximations, using Thomas-Fermi or Lenz-Wentzel potentials [6-11]. We will only consider the "exact" calculations which use the best available atomic ground state wave functions and partial wave expansions to calculate the differential cross sections. The particular sources used for the cross section calculations are Schafer et al [12] for small angles and Lin [13] for large angles.

Recent scattering experiments using thin films and gas phase targets are in good agreement with these calculations.

The experiments cited are Motz et al [14] for foil measurements and Kessler and Weichert [15] for gas phase measurements. Kessler and Weichert normalized to carbon, but Moore and Fink [16] were able to convert to absolute cross sections.

There are some reasons to expect that cross sections measured in a microscope might not be the same as the accepted cross sections.

Perhaps the biggest difference between the microscope measurements and other methods is the hugely different beam intensities. In foil or gas measurements, no atom will see more than one electron, and most never see any electrons. Elastic scattering is ensured by energy discrimination in which only primary energy electrons are counted. This means that the gas and foil measurements are made on atoms in a ground state that scatter one electron.

The microscope used in this experiment can produce a 50 kv beam of 4×10^9 electrons/sec (6.4×10^{-10} amp) in a focused spot of 2.8 Å diameter which gives an intensity of 5.2×10^{10} watts/cm^2. (The surface of the sun, for comparison, is 6.3×10^3 watts/cm^2.)

The microscope normally scans an area 290 Å by 290 Å in 17 seconds. The theoretical elastic cross section for Uranium is .5 Å^2. This means that $4 \times 10^9 \times 17 \times .5/290^2 = 4 \times 10^5$ elastic events occur for each Uranium atom in the scanned area for each full scan.

We can easily show that the microscope measurements are made on atoms that are at least in a singly excited state on the average. A typical atomic excited state has a 10^{-8} sec lifetime. Metastables and typical Uranium compounds [17,18] have 10^{-4} to about 10^{-3} sec lifetimes. Even ignoring the compounds and metastables, the atom will still be in an excited state when the next electron probes its potential. We can estimate further on this excitation. The ratio $\sigma_{\text{inelastic total}}/\sigma_{\text{elastic total}}$ is about 20/Z [9]. For Uranium, the number of inelastic events is therefore about 9×10^4 per atom per picture.

Using 10^{-8} sec as the average lifetime, 6 Å^2 as the beam area, and 0.5 Å^2 as the total elastic cross section, each time the beam scans across

the atom, $\frac{20}{92} \times 4 \times 10^9 \times \frac{0.5}{6} T = 0.72 \times 10^8 T$ inelastic events occur, where T is the time that the beam is on the atom (0.17×10^{-3} sec). We can expect that $0.72 \times 10^8 T \times 10^{-8}/T = 0.72$ would be the approximate probability that the atom is in an excited state while the beam is over the atom. Therefore the atom is on the average in a singly excited state during the measurement.

In addition, recoil motion of the atoms might influence the cross section determination. It is conceivable that while undergoing 5×10^5 collisions, the heavy atoms might be systematically deflected away from the beam. A few Angstroms would make a significant difference. These are a few effects out of the large number of possible interactions between the atoms, beam, carbon film support, and the 25 kgauss magnetic field from the lens at the specimen.

For these reasons, there is ample reason to suspect that the cross sections observed in a microscope might differ from the accepted cross sections.

In addition to the physical interest in this experiment, there is an important practical reason to make this measurement. The ability to see and locate single heavy atoms should allow their use as labels on biological molecules. Such a technique could be of great practical importance, but only if the heavy atoms can be identified with a high efficiency and located with precision. The measurement of cross sections would furnish some useful information about single atom identification in a microscope. Some discussion will be presented concerning the experimental factors which limit atomic-number resolution.

II. DESCRIPTION OF MICROSCOPE

The microscope used in this experiment is a field emission scanning transmission electron microscope [19] designed and constructed at the University of Chicago. The microscope has two magnetic lenses and is designed for 100 kv operating voltage. This experiment, however, was performed at 50 kv.

As shown in Fig. 1,

the electron source is a field emission tip which is at negative high voltage. The next element is an electrostatic lens of the Butler type [20] designed for minimum spherical aberration. The first anode is one cm from the tip and 4.5 kv positive relative to the tip. The second anode is grounded and 3 cm from the first anode. With this particular geometry, the beam emerges from the gun slightly diverging and is collimated by a condenser lens 13 cm from the first anode. An aperture defines the beam size to a chosen value, and the beam is focused by the objective lens onto the specimen. The specimen is inside the objective lens, and the objective is shown in Fig. 1 as two separate lenses, one above and one below the specimen. The principal plane of the objective is 40 cm from the first anode, and the focal length of the objective is about 1 mm.

The beam is scanned over the specimen by double deflection coils between the aperture and the objective. An astigmatism corrector is located between the first and second deflection coils.

The electrons that have passed through the thin specimen are collected by two detectors. The solid detector collects all electrons within an angle β_{min} (measured at the specimen) from the optical axis. The annular detector collects all electrons which leave the specimen between the angles β_{min} and β_{max}.

The detectors are silicon surface barrier types supplied by the Laboratory for Astrophysics and Space Research of The University of Chicago.

The vacuum requirements for stable operation of the field emission tip are far more stringent than for any other part of the microscope, so there are two separate vacuum levels separated by a low conductance beam tube. This tube passes through the condenser lens and has a conductance of 0.5 l/sec. The tip section operates in the 10^{-10} or 10^{-11} Torr region, and the specimen section is in the 10^{-9} level.

Specimens are changed with a double air lock type specimen changer where the specimens can also be baked at roughly 100°C and 10^{-8} Torr. This is useful in preventing specimen contamination while it is in the beam [21].

The machine was designed to ultimately obtain 1 Å resolution, so the power supplies were built to provide a stability sufficient to operate at that required level. The high voltage [19], the current supplies [22] for the magnetic lenses, and the DC part of the beam deflection circuit all operate at a stability of one part per million per hour.

One problem that can affect the experiment is the AC level of the ambient magnetic field. The horizontal scan of the microscope is synchronized to 60 hz so that an external AC field will show up as local variations in the magnification and thereby cause some distortion but will not produce large visible oscillations. By extensive internal and external shielding and an electrical feedback circuit, this distortion is held to 10 per cent at 290 Å full scale scan. Mechanical vibration and distortion make this the maximum useful magnification. The deflection is digital, normally 17 seconds for a 1024 by 1024 element picture, and the detector signals are displayed for

focusing on a scan converted television display [23]. Micrographs are taken in a remote camera system by photographing a precision cathode ray tube which is scanned synchronously with the microscope and intensity modulated by the detector output.

The specimen consists of a copper or gold microscope grid, supporting a holey collodian film, which further supports a carbon film 10 to 20 Å thick. A dilute solution of the element to be measured is applied to the carbon film as described in the literature [21]. The concentration is sufficient to leave about 10 to 200 separate heavy atoms on the 290 Å full scale field of view. To obtain high resolution, the microscope must be properly aligned, and careful procedures were established to produce this alignment. Once aligned, most of the aberrations which could limit resolution are significantly reduced.

The only important surviving terms contributing to the finite resolution are the demagnified source size, spherical and chromatic aberrations of the objective lens, and diffraction. Spherical aberration and diffraction both depend on the beam diameter. Wave optical calculations [24] indicate that the optimum resolution using the beam diameter or equivalently α, the beam convergence half angle at the specimen, as a variable occurs at $\alpha_{optimum} = 1.4\ (\lambda/C_s)^{1/4}$. λ is the electron wavelength and C_s is the spherical aberration coefficient of the objective lens. With this optimum angle, the resolution is .6 λ/α plus the source size and chromatic aberration terms (.6 λ/α = 2.3 Å, λ = .0534 Å, C_s = .55 mm, α_{opt} = .0139).

For the geometry described here, the source size term is about 10 Å [25], demagnified 80 times or .1 Å; chromatic aberration of the objective is 0.4 Å; and the resultant resolution, combining the three terms in quadrature, is 2.3 Å. Atoms 2.8 Å apart have been experimentally resolved.

The actual shape of the focused spot is important. If we consider only diffraction, the shape is an Airy disk. The intensity outside the central peak of an Airy disk is 16 per cent of the total. When spherical aberration is included at the optimum angle and the focus is adjusted slightly, the resulting shape is a modified Airy disk. The full width at half maximum is unchanged, but the peak intensity is reduced to 78 per cent, and 33 per cent of the total intensity is now outside the central peak.

A parameter which will be shown to be important to this experiment is the fraction of the beam that occurs within 4 Å of the center of the focused spot. This depends on the actual angle α used and the sharpness of focus. Best focus is defined here as the condition where the current density is at maximum. Fig. 2 shows the fraction of the beam inside a 4 Å radius circle at best focus as a function of α. Fig. 3 shows how the fraction depends on the focus at $\alpha = \alpha_{optimum}$. Figs. 2 and 3 are based on calculations made using a computer program written by V. Beck.

III. DESCRIPTION OF EXPERIMENT

Cross sections are defined by the relation $I_{scat} = \sigma J$ where I_{scat} is the scattered current, σ is the cross section, and J is the incident current density. The output of the annular detector as the beam is scanned over the specimen is proportional to

$$\int_{\beta_{min}}^{\beta_{max}} \frac{d\sigma}{d\Omega} 2\pi \sin\theta d\theta = \sigma_{collected}$$

at each point on the specimen. The proportionality constant is the current density of the focused beam, which is unchanged during the exposure.

σ_{coll} is the differential cross section integrated over the full azimuthal angles and between β_{min} and β_{max} in scattering angle. β_{min} is a strong function of specimen height, and β_{max} is 5.4 x β_{min} plus a spherical aberration correction. The factor of 5.4 is the ratio of the annular detector outer diameter to the hole diameter.

The object of the experiment is to measure σ_{coll} absolutely over a large range of β_{min} (about .02 to .2 radians). This can then be compared to the calculated differential cross sections integrated similarly.

We will now consider how this signal can be stored and retrieved and the cross section information extracted. I_{scat} is converted to a voltage by an electrometer and sent to the TV display and to the camera system.

A photographic technique was developed which can store analog information linearly if the signal fluctuation is less than 30 per cent of our usual black to white range. Because of brightness limitations in our camera system, a very fast film, Royal X 120, was used. The film was developed with DK 50 at 68°F for 8 minutes. The optical transmission of the film was measured with a manual spot densitometer of our design. The densitometer consists of a commercial enlarger [26] and a movable screen at the film's focus with a 4 mm diameter hole and a CdS photocell beneath the hole. The hole was covered with a diffusing material and the resistance of the photocell was measured with a 4-1/2 digit digital ohmmeter.

The enlarger was set to focus the film, which was a micrograph 290 Å full scale, to a 14.5 cm full scale image. The 4 mm hole was then 8 Å in diameter on the micrograph. The 8 Å diameter hole size was chosen as a compromise between collecting as many scattered electrons as possible and still being able to sense local fluctuations in the carbon film thickness.

At f/11, where the densitometer was calibrated, there is a center-to-edge brightness variation of about 1 f stop. This is due to the enlarger alone, and is easily eliminated by a calibration curve.

To calibrate the system, test voltages were applied to the camera system and DC levels photographed. After the film was processed, the densitometer conductivity was plotted against the test voltages. The conductivity was first corrected for center-to-edge variations. At low signal levels, the response was limited by film fog, and at high levels the film saturated. Over about 30 per cent of the normal black to white range the response was linear and repeatable. Once calibrated, the densitometer gave the signal that was at the annular detector output while the micrograph was taken, averaged over an 8 Å diameter area.

The film grain size is about 20 μ [27], and a 3 Å spot is 600 μ on the film, so the grain is insignificant.

To subtract the carbon film background, a measurement was first made with the densitometer over the atom spot. Then a number of measurements were made at points surrounding the atom, and the average of these was subtracted from the level over the atom.

To convert this to a cross section, the following derivation is presented. It is based on a derivation by Wall [28]. On the specimen the current density at (x_1, y_1) of the focused beam is $J(x_1-x_2, y_1-y_2)$ when the beam is centered at (x_2, y_2). The cross section σ is defined by $I_{scat} = \sigma J$. Since we use a digital scan system, the scattered current $I_{scat}(ja, ka)$, where $\underset{\sim}{a}$ is the scan increment and $\underset{\sim}{j}$ and $\underset{\sim}{k}$ are integers, can be expressed as

$$I_{scat}(ja, ka) = \sum_i J(ja-x_i, ka-y_i)\, \sigma(x_i, y_i).$$

σ_i is the cross section of the i^{th} atom which is located at (x_i, y_i). $I_{scat}(ja, ka)$ is the scattered current while the beam is centered at (ja, ka).

Summing both sides over j and k, and because the sums are finite, we can interchange the order of summation on the right hand side. The sums are over the entire scan so j and k range from -512 to +512.

$$\sum_{j,k} I_{scat}(ja, ka) = \sum_{i} \sigma_i(x_i, y_i) \sum_{j,k} J(ja-x_i, ka-y_i).$$

But since

$$\sum_{j,k} a^2 J(ja-x_i, ka-y_i) = I_o$$

where I_o is the incident beam current,

$$\sum_{j,k} I_{scat}(ja, ka) = \sum_{i} \sigma_i(x_i, y_i) \frac{I_o}{a^2}.$$

For only one atom,

$$\sum_{j,k} I_{scat}(ja, ka) = \sigma \frac{I_o}{a^2}$$

or

$$\sigma = \frac{a^2}{I_o} \sum_{j,k} I_{scat}(ja, ka).$$

The densitometer measures an area which here is assumed larger than the atom image and after the carbon film had been subtracted, produced a signal which is the average value of I_{scat} over the 8 Å hole.

$$\text{Densitometer output} = \frac{\sum_{\text{hole}} a^2 I_{scat}(ja,ka)}{\sum_{\text{hole}} a^2} = \frac{\sum_{\text{all } j,k} a^2 I_{scat}(ja,ka)}{\text{hole area}},$$

because I_{scat} is zero outside the densitometer sampling hole. The result is

$$\sigma_{coll} = \frac{\text{densit. output x hole area}}{I_o}.$$

I_o is measured with the solid detector.

We are convinced that single atoms are seen, and as evidence we offer a histogram. Fig. 4 shows the grouping of data on a uranium specimen on which 135 spots were measured. The singles and doubles peaks are apparent.

Also, what may be more convincing to us are the hundreds of micrographs that we have taken where single, round, bright spots appear. We show a few such micrographs in Figs. 5, 6 and 7.

The repeatability of cross section measurements is 5 per cent for repeated measurements of the same spots on the same exposure. This fluctuation is due to slight variations in the positioning of the densitometer hole relative to the atom image and possibly small variations in the densitometer response.

However, measurements of the same atoms on different exposures have a larger variation. This type of test shows a repeatability of 30 per cent.

We believe that this additional 25 per cent, which shows up in almost all the data, is due to several factors, among which are focus variations, atom motion, beam vibration, and scan distortion. More will be said about this later.

Detector linearity with current can be demonstrated by two experiments. First we can establish linearity over a range of 50 in beam current from the highest beam current down to 2 per cent of the highest beam current by changing aperture diameters that define the beam. The microscope has three

apertures in the approximate area ratio of 1:6:25. By changing apertures as the beam current slowly drops after tip flashing [29], we can increase the range over a factor of 50 from the highest readable current. The linearity has been established for this range as 9.5 $\pm$ 9.1 per cent.

A separate experiment is necessary to explore the low current response. We used the scattered electrons from a rolled-up carbon film and obtained scattering intensities from multiples of one carbon film thickness. In this way, linearity has been established in the 0.5 to 2 per cent range of the highest beam, within about 5 per cent.

The other important detector property is frequency response. This can be established by scanning over a hole in the carbon film and examining the video output as the scan size is increased. In this way, the frequency response of the detectors and amplifiers has been established as flat out to beyond 15 khz. This is sufficient to pass all spatial frequencies of the modified Airy disk without attenuation. Both the annular and solid detectors have the same response.

IV. CALIBRATION OF MICROSCOPE

There are three important microscope parameters that must be known for this experiment. They are the magnification and the inner and outer angles of scattering collection. In addition, since we wanted to measure the collected cross sections at various collection angles, we needed to calibrate the three parameters over a wide range of specimen heights or equivalently objective currents for focus. The specimen height has a radical effect on the collection angles because at one height the unscattered beam can be refocused at the annular detector plane corresponding to a very large β_{min}, while at

a slightly different height the unscattered beam will just fill the hole in the annular detector. This corresponds to β_{min} equal to the beam angle at the specimen or α, which is the smallest usable β_{min}.

The scan magnification was calibrated with a diffraction grating replica over a range of 1.7:1 in focus current without about 50 individual measurements.

The calibration of β_{min} vs. objective current is a two-step operation. First we can measure the ratio of β_{min}/α. This is simply the number of times the unscattered beam will fit inside the annular detector hole. A correction for the spherical aberration of the lens below the specimen must be considered, but will be ignored in the discussion. The ratio β_{min}/α was measured by scanning the unscattered beam below the objective lens with the lower scan coils. The convolution of the beam with the detector yields β_{min}/α directly. Care was taken to insure that astigmatism was not important. Calibrating α is more difficult, especially since over the large current range used the lens goes in and out of saturation. This causes the principal planes to shift position in a non-uniform fashion. An unambiguous method was developed. Consider the first order properties of the lens in matrix form. The most general transfer matrix for a thick lens is

$$M = \begin{pmatrix} a & b \\ c & d \end{pmatrix}, \text{ with } |\det M| = 1.$$

For this lens to focus a beam of radius R_o and convergence angle E on the specimen,

$$\begin{pmatrix} a & b \\ c & d \end{pmatrix} \begin{pmatrix} R_o \\ E \end{pmatrix} = \begin{pmatrix} 0 \\ \alpha \end{pmatrix}.$$

This means that

$$M = \begin{pmatrix} \frac{E}{\alpha} & \frac{-R_o}{\alpha} \\ \frac{\alpha - Ed}{R_o} & d \end{pmatrix}.$$

Now we consider a single scan operating condition, in which the deflection coil is outside the lens field and a distance L away from the principal plane (L >> focal length). With a half scan angle of γ,

$$\begin{pmatrix} \frac{E}{\alpha} & -\frac{R_o}{\alpha} \\ \frac{\alpha - Ed}{R_o} & d \end{pmatrix} \begin{pmatrix} L\gamma \\ \gamma \end{pmatrix} = \begin{pmatrix} \text{1/2 field of view (FOV)} \\ \text{angular magnification term} \end{pmatrix}.$$

This gives an expression for α in terms of the measurable quantities γ, E, L, R_o and FOV

$$\alpha = \frac{\gamma(EL - R_o)}{1/2\ FOV}.$$

The beam is virtually parallel entering the lens, so EL << R_o, and we estimate a 5 per cent uncertainty in calibrating each of γ, R_o, and FOV. Then allowing 5 per cent in the convolution measurement of β_{min}/α, β_{min} is known to $\pm$ 20 per cent.

Up to a few hundred milliradians, third order optical theory is sufficient to calculate β_{max}. For the larger angles, a non-paraxial ray tracing technique was used.

To summarize, we estimate the magnification to be known to $\pm$ 5 per cent, β_{min} to $\pm$ 20 per cent, and β_{max}/β_{min} to $\pm$ 5 per cent. Since the cross sections depend on the magnified area of the densitometer hole, combining magnification uncertainty and distortion, the maximum bias in the cross section data is $\pm$ 20 per cent.

V. DATA

Techniques for specimen preparation and controls are described in the literature [21]. Data were obtained on specimens of Hg, Ag, and U at 50 kv. The specimens were provided by J. Langmore. Pictures were taken over a wide range of β_{min} by varying the specimen height.

The data are plotted in Fig. 8 as collected cross sections vs. β_{min}. Each data point represents 15 to 100 atom measurements. On the same graph, the theoretical cross sections are shown in equivalent form as

$$\int_{\beta_{min}}^{\beta_{max}} \frac{d\sigma}{d\Omega} 2\pi \sin\theta d\theta,$$

where $d\sigma/d\Omega$ was obtained from the literature [12,13]. The calculations were interpolated to 50 kv and to the elements for which calculations were not available. To better represent the physical situation in the microscope, the theoretical curves were convoluted with the incoming beam angle of $\pm \alpha$.

The data are presented with the maximum biases added in the error bars. The data were collected over a range of α ($\alpha_{optimum} \pm 20$ per cent) and corrected by the fraction of the beam lost outside the densitometer hole using Fig. 2.

We could experimentally distinguish silver atoms from mercury or uranium but not between the two heavier atoms. The calculated σ_{coll} for Mercury or Uranium is at least 70% larger than for Silver, which allows us to distinguish Silver from the other two. Uranium and Mercury differ by less than 30%, which is within the experimental error. In total about 600 separate cross section measurements were made in this experiment.

VI. DISCUSSION

compared to theory,

The data is low on the average/with the calculated values just inside the combined standard deviation and bias bars. Relative to the error bars, the average discrepancy is small. It is possible that this consistent discrepancy may be due to the fact that we have ignored the finite source size, chromatic aberration, and the finite size of the atom in calculating the intensity contained in the region outside a 4 Å radius from the center of the spot. About one-third of the experimental standard deviation can be explained using Fig. 3. Slight variations in the sharpness of focus will cause the intensity inside the 4 Å radius hole to vary. Experimentally, it is difficult to set the focus current to the exact point of the peak in the modified Airy disk. It is estimated that the focus can be repeatably found so that the peak current density is within 60 per cent of the maximum. Assuming a random distribution in data taken at focus settings with the peak $\geq$ 60 per cent of the maximum, a standard deviation of 8 per cent in the data would result. The remainder of the standard deviation presumably comes from the densitometer measurements, scan distortion, beam vibration, and atom motion. The probable distribution of the sources of the standard deviation is: densitometer measurements 5 per cent, focus variations 8 per cent, scan distortion 10 per cent, and 7 per cent from beam vibration and atom motion.

Ionization of the atoms is possible, but calculations [11] on doubly ionized mercury show that the scattering is different only inside of about .02 radians. The data reported here are for angles larger than .02 radians, and so it should not be important.

There are some data regarding a possible dose rate or current level effect. At the operating conditions used in this experiment, the beam current may be varied by a factor of 4. Cross section measurements did not vary, within the standard deviation, with a change of a factor of 4 in the beam current.

Since there is no energy filtering in this experiment, we must consider the inelastic contribution to the cross section measurements. An estimate was made using the energy loss spectra of Daniels [30] for 60 kv electrons incident on silver. The worst case is for the lowest Z (silver) and smallest angles (.030 to .035 radians). In that angular range, 3 per cent of all inelastic events occur, which makes a cross section of $0.03 \times 0.1 \times (20/47) = 0.0013$ Å^2. The measured cross section in that range is 0.01 Å^2. Inelastic collisions amount to, at most, 13 per cent of the measurements.

The measurements were not corrected for the inelastic contribution because Hg and U energy loss data was not available, and the effect is small compared to the experimental biases.

VII. CONCLUSION

It appears that the experimentally observed brightness of single atom images can be reconciled with the theoretical descriptions of electron-atom scattering and other experimental observations. However, the brightness of the spots is considerably less than would be observed on naive assumptions. The effect of the spherical aberration of the lens both in the upper half (where the focused spot is formed) and in the lower half (which determines the collecting power of the detectors) is considerable, reducing the anticipted

brightness by a factor of two or so. This effect must be taken into account in determining which atoms will be visible in a specimen when using a scanning transmission electron microscope.

In addition, we have verified that the effect of ionization and excitation of the atoms on the scattered intensity is small and that in spite of the enormously high scattering intensity (10^6/atom) the effect of atomic recoil or motion during the exposure is small.

VIII. ACKNOWLEDGEMENTS

This experiment has made extensive use of the technology recently developed concerning field emission scanning electron microscopes. We would like to acknowledge the essential contributions of Prof. A. V. Crewe, the principal investigator, and his students, staff, and colleagues in the microscope group. In particular, W. Mankawich was responsible for the mechanical design and fabrication of the microscope, and useful discussions were had with Prof. M. Isaacson, Dr. J. Wall, and Prof. E. Zeitler, in addition to those already mentioned.

REFERENCES

1. A. V. Crewe, J. Wall and J. Langmore, Science 168, 1338 (1970).

2. R. M. Henkelman and F. P. Ottensmeyer, Proc. Natl. Acad. Sci. (USA) 68, 3000 (1971).

3. H. Hashimoto, A. Kumao, K. Hind, H. Yotsumoto and A. Ono, Jap. J. Appl. Phys. 10, 1115 (1971).

4. F. Thon and D. Willasch, Optik 36, 55 (1972).

5. J. Wall, J. Langmore, A. V. Crewe and M. S. Isaacson, Proc. Natl. Acad. Sci. (USA) 71, 1974). In press.

6. N. F. Mott and H. S. W. Massey, The Theory of Atomic Collisions, 3rd Ed. (Clarendon Press, Oxford, England, 1965).

7. L. H. Thomas, Proc. Cambridge Phil. Soc. 23, 542 (1926).

8. E. Fermi, Zeit. Physik 48, 73 (1928).

9. F. Lenz, Zeit. Naturforsch. 9A, 185 (1954).

10. G. Wentzel, Zeit. Physik 40, 590 (1927).

11. J. P. Langmore, J. Wall and M. S. Isaacson, Optik 38, 335 (1973).

12. L. Schafer, A. C. Yates and R. A. Bonham, J. Chem. Phys. 55, 3055 (1971).

13. S. R. Lin, Phys. Rev. 133, 965 (1964).

14. J. W. Motz, R. C. Placious and C. E. Dick, Phys. Rev. 132, 2558 (1963).

15. J. Kessler and N. Weichert, Zeit. Physik 212, 48 (1968).

16. P. Moore and M. Fink, Phys. Rev. A 5, 1747 (1972).

17. G. H. Dieke and A. B. F. Duncan, Spectroscopic Properties of Uranium Compounds (McGraw-Hill, 1949).

18. G. R. Harrison, R. C. Loro and J. R. Loofbourow, Practical Spectroscopy (Prentice-Hall, 1948).

19. A. V. Crewe and M. W. Retsky, Proc. 30th Ann. EMSA Conf., 472 (1972).

20. J. W. Butler, Proc. 6th International Conference for Electron Microscopy, 191 (1966).

21. M. Isaacson, J. Langmore and J. Wall, Scanning Electron Microscopy, 1974, IITRI, Chicago, Illinois (in press).

22. M. W. Retsky and J. Wall, Rev. Sci. Inst. 43, 384 (1972).

23. V. Beck, Rev. Sci. Inst. 44, 1064 (1973).

24. M. S. Haine, The Electron Microscope (E. and F. N. Spon, London, 1961).

25. A. V. Crewe, Progress in Optics XI edited by E. Wolf (North-Holland Publishing, Amsterdam, 1973).

26. Omega Type D2 Enlarger with a type D condenser lamphouse.

27. Kodak Publication No. AF-13.

28. J. Wall, Ph.D. Thesis, The University of Chicago (1971).

29. A. V. Crewe, M. Isaacson and D. Johnson, Rev. Sci. Inst. 41, 20 (1970).

30. J. Daniels, Zeit. Physik 227, 234 (1969).

FIGURE CAPTIONS

Fig. 1. Electrons are drawn from the tip by field emission and the beam leaves the gun slightly diverging. The beam is collimated by the condenser lens and defined in size by the defining aperture. The electrons are focused by the objective lens onto the specimen which is in the center of the lens field. The objective lens is shown as two separate lenses so that angles at the specimen are more obvious. The half convergence angle at the specimen is α. The solid detector collects all electrons within an angle β_{min} and the annular detector collects the electrons which leave the specimen between β_{min} and β_{max}. The beam is scanned over the specimen by the double deflection coils located between the aperture and objective.

Fig. 2. $\int_0^{4\text{Å}} J(r)\, 2\pi\, r\,dr \Big/ \int_0^{\infty} J(r)\, 2\pi\, r\,dr$ as a function of the beam convergence angle at the specimen at optimum focus. J(r) is the current density of the beam when centered at r = 0.

Fig. 3. The horizontal scale is in units of $\alpha^2\ \Delta f/2\lambda$, where Δf is the focus change from the gaussian focus. The solid curve is J(0), the current density at the center of the beam, in relative units as a function of focus. Optimum focus or maximum J(0) occurs at 1 wavelength defocus. One wavelength defocus corresponds to about 500 Å in the axial direction or about 7 ppm in objective lens current. The dashed curve shows $\int_0^{4\text{Å}} J(r)\, 2\pi\, r\,dr$ as a per cent of the total beam current as a function of focus.

Fig. 4. A histogram showing the distribution in σ_{coll} data for a uranium specimen. The peaks corresponding to single atoms and doubles are apparent. The measurements included spots that were obviously not single atoms.

Fig. 5. A micrograph of uranium where the single U atoms are seen as bright spots. The brightness of the atom images depends on the thickness of the underlying carbon film support, the variation of which is apparent. The scan size is 290 Å full scale.

Fig. 6. A 290 Å full scale micrograph of mercury atoms. The Hg images are similar in brightness to the uranium images in Fig. 5.

Fig. 7. A print from a linear negative of silver atoms. The vertical scan size is 290 Å. The Ag atoms show up substantially reduced in brightness compared to Hg or U. The large clusters were not on the specimen before the silver was added and are unidentified. Silver is close to the limit where single atoms are obvious compared to the carbon film structure for these operating conditions.

Fig. 8. The collected cross sections (σ_{coll}) in the form of

$$\int_{\beta_{min}}^{\beta_{max}} \frac{d\sigma}{d\Omega}\, 2\pi \sin\theta \, d\theta$$

for U, Hg, and Ag atoms. The theoretical curves are shown in the same form. The error bars include maximum biases of 20% in σ_{coll} and in β_{min}.

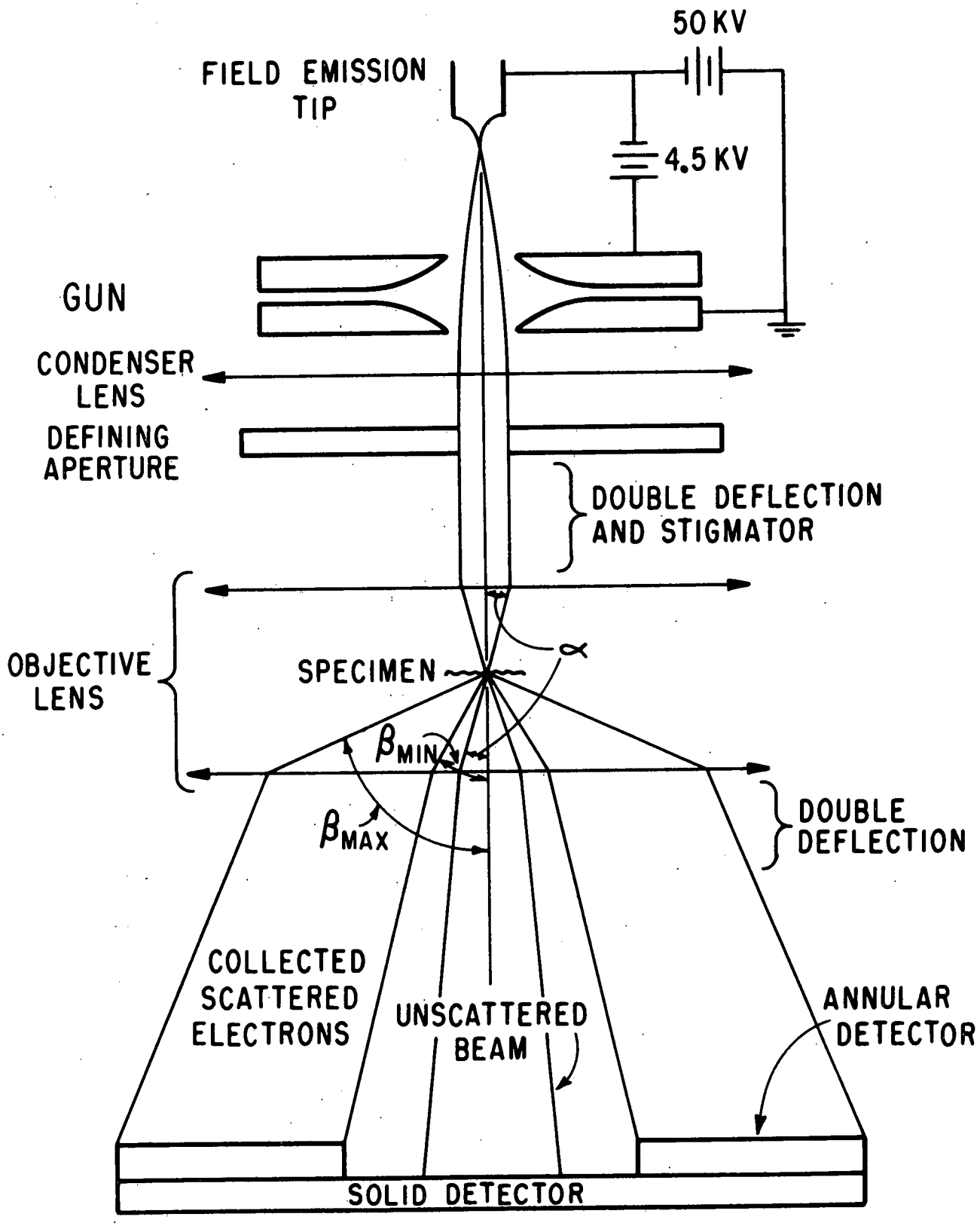
50 KV
FIELD EMISSION TIP
4.5 KV
GUN
CONDENSER LENS
DEFINING APERTURE
DOUBLE DEFLECTION AND STIGMATOR
OBJECTIVE LENS
SPECIMEN
α
β_{MIN}
β_{MAX}
DOUBLE DEFLECTION
COLLECTED SCATTERED ELECTRONS
UNSCATTERED BEAM
ANNULAR DETECTOR
SOLID DETECTOR

Fig. 1

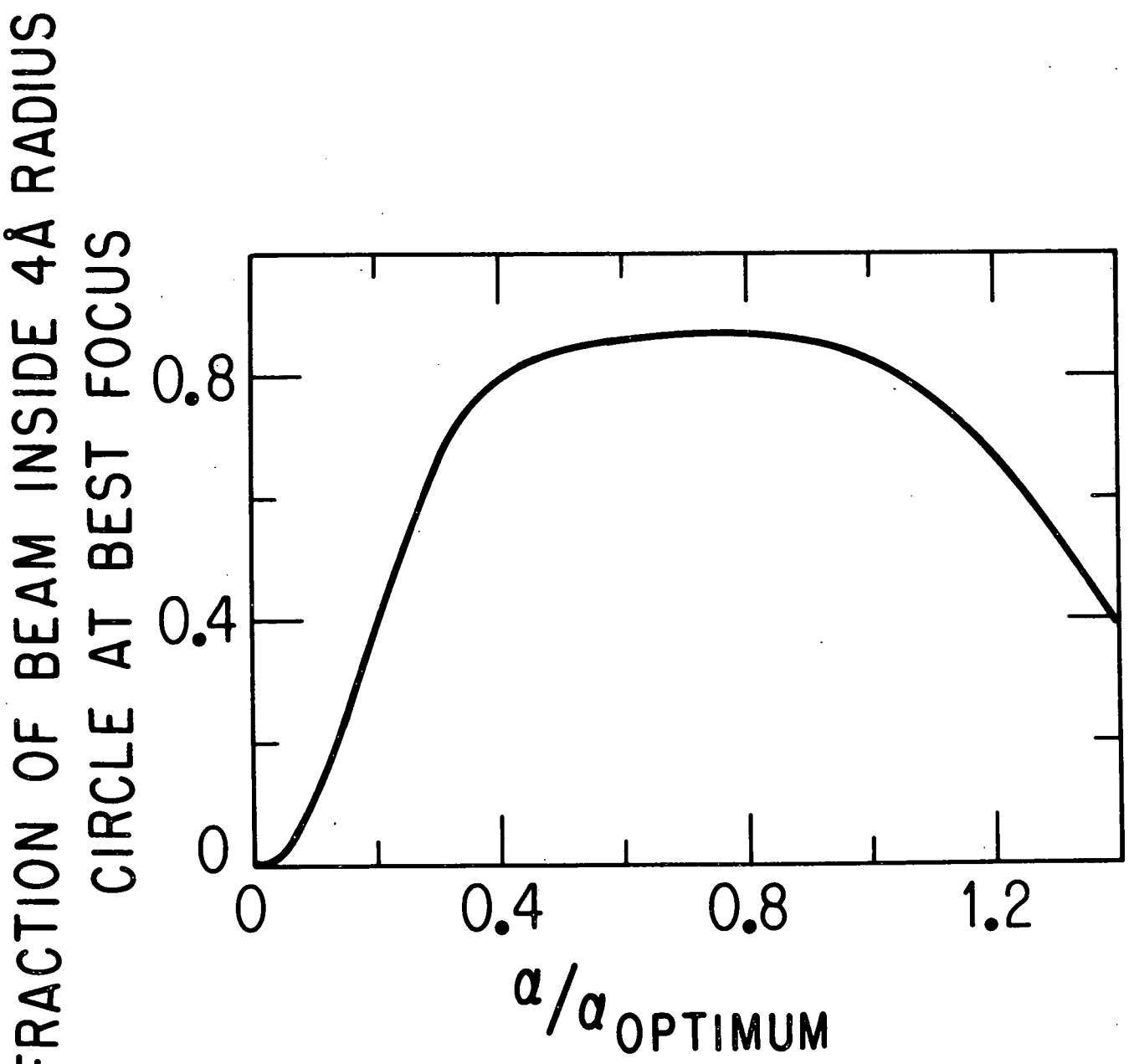
FRACTION OF BEAM INSIDE 4Å RADIUS CIRCLE AT BEST FOCUS
0.8
0.4
0
0
0.4
0.8
1.2
α/α OPTIMUM

Fig.2

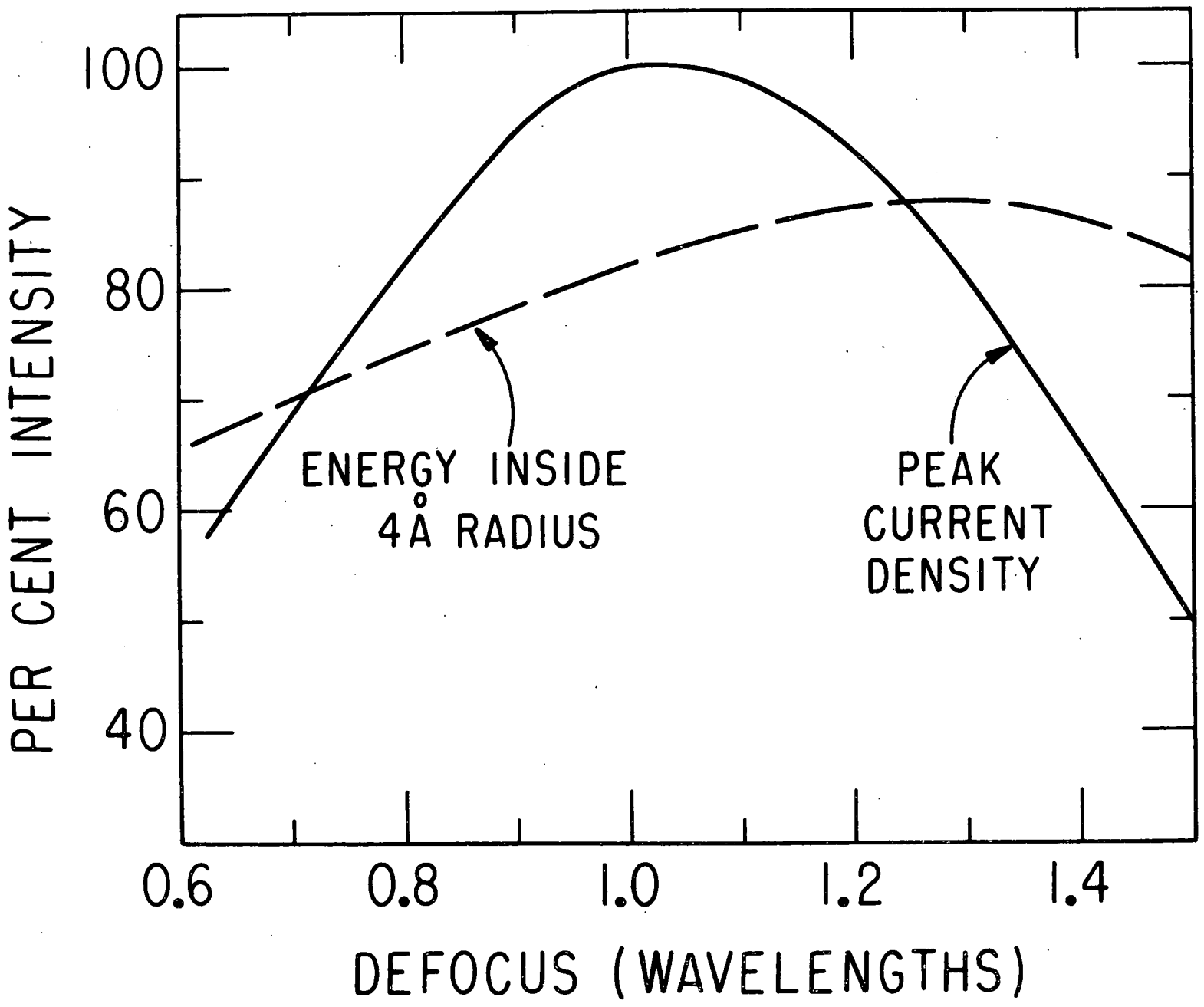
100
80
60
40
PER CENT INTENSITY
ENERGY INSIDE
4Å RADIUS
PEAK
CURRENT
DENSITY
0.6
0.8
1.0
1.2
1.4
DEFOCUS (WAVELENGTHS)

Fig.3

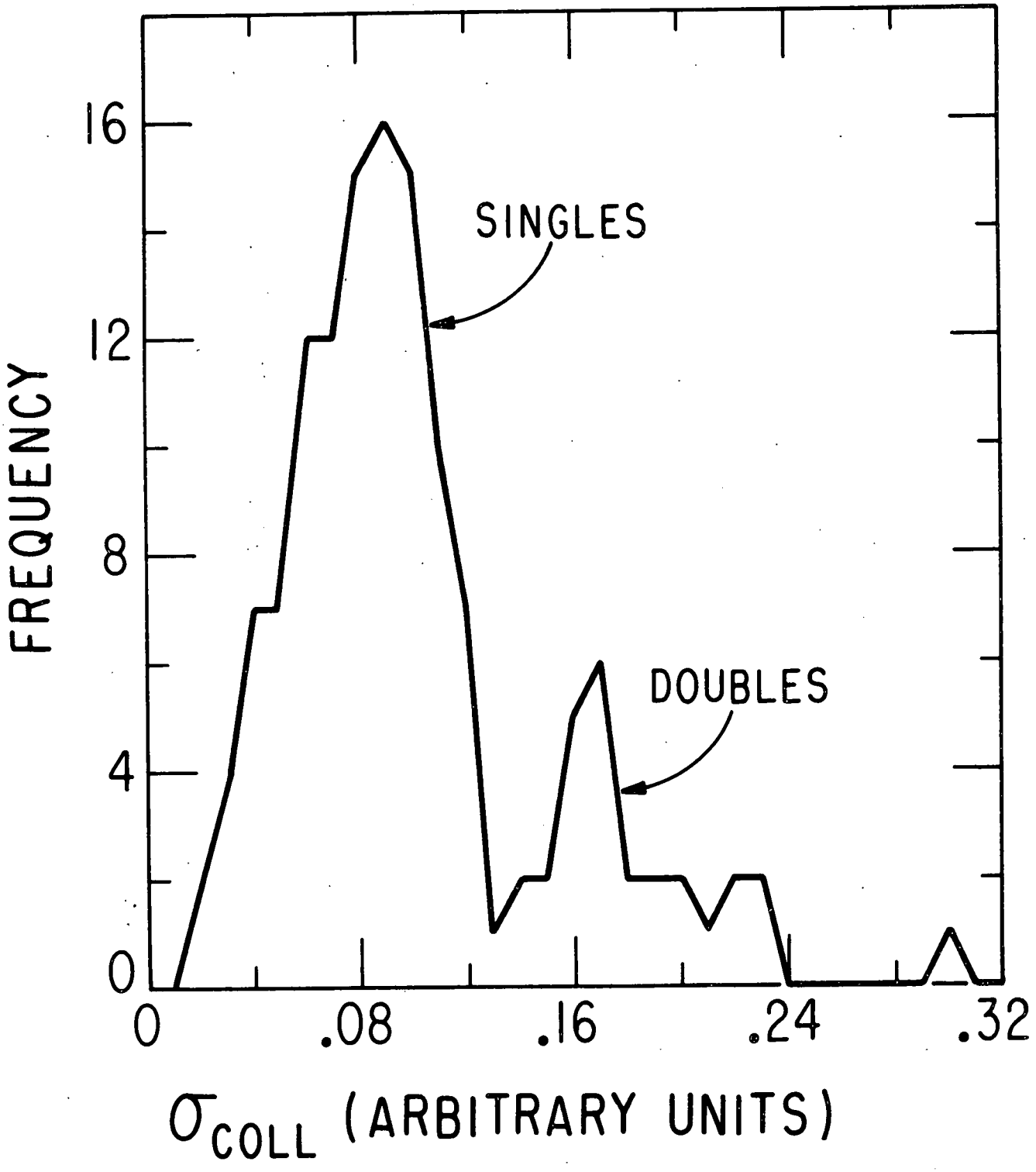
16
12
8
4
0
FREQUENCY
SINGLES
DOUBLES
0
.08
.16
.24
.32
σ_{COLL} (ARBITRARY UNITS)

Fig.4

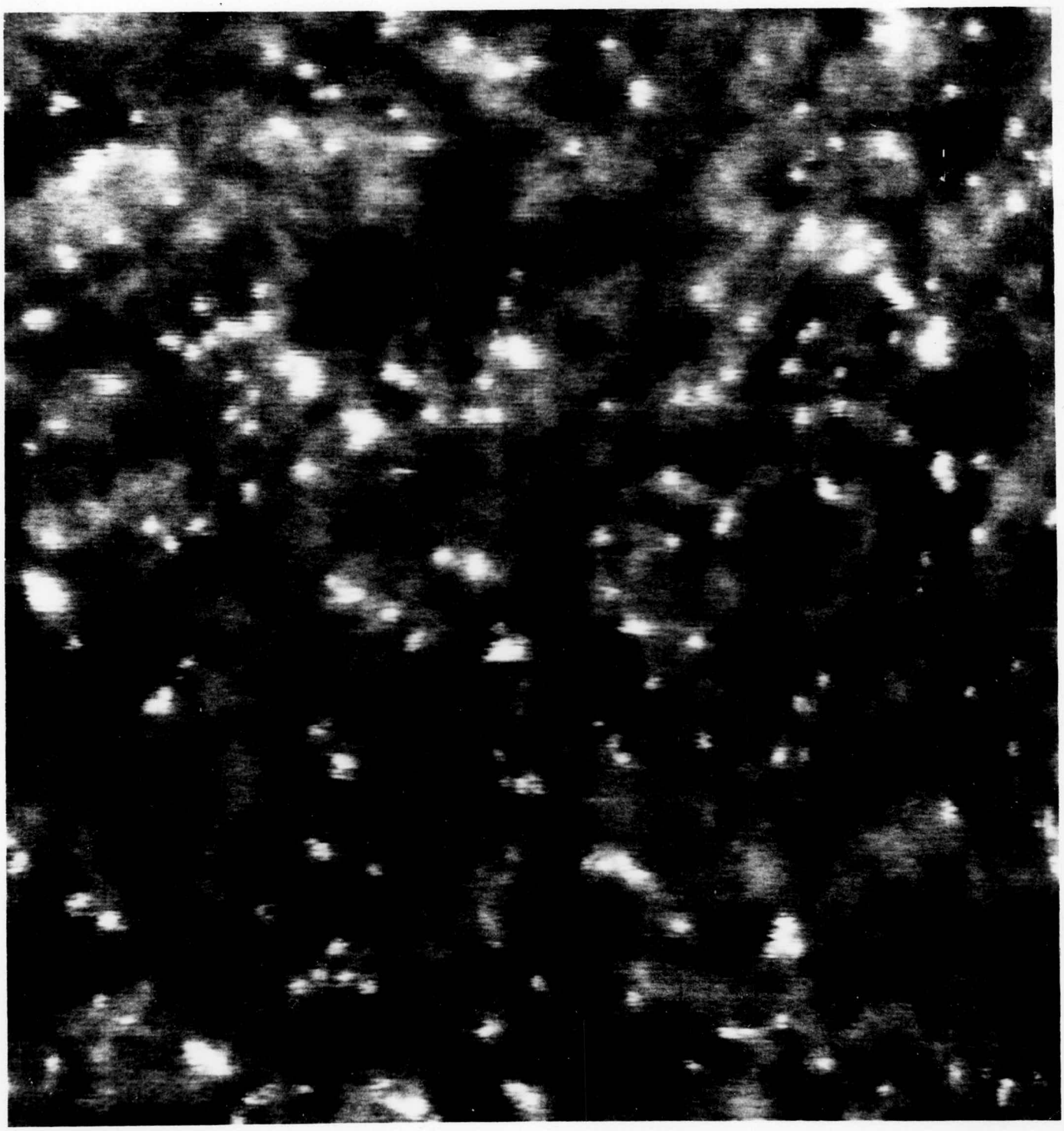

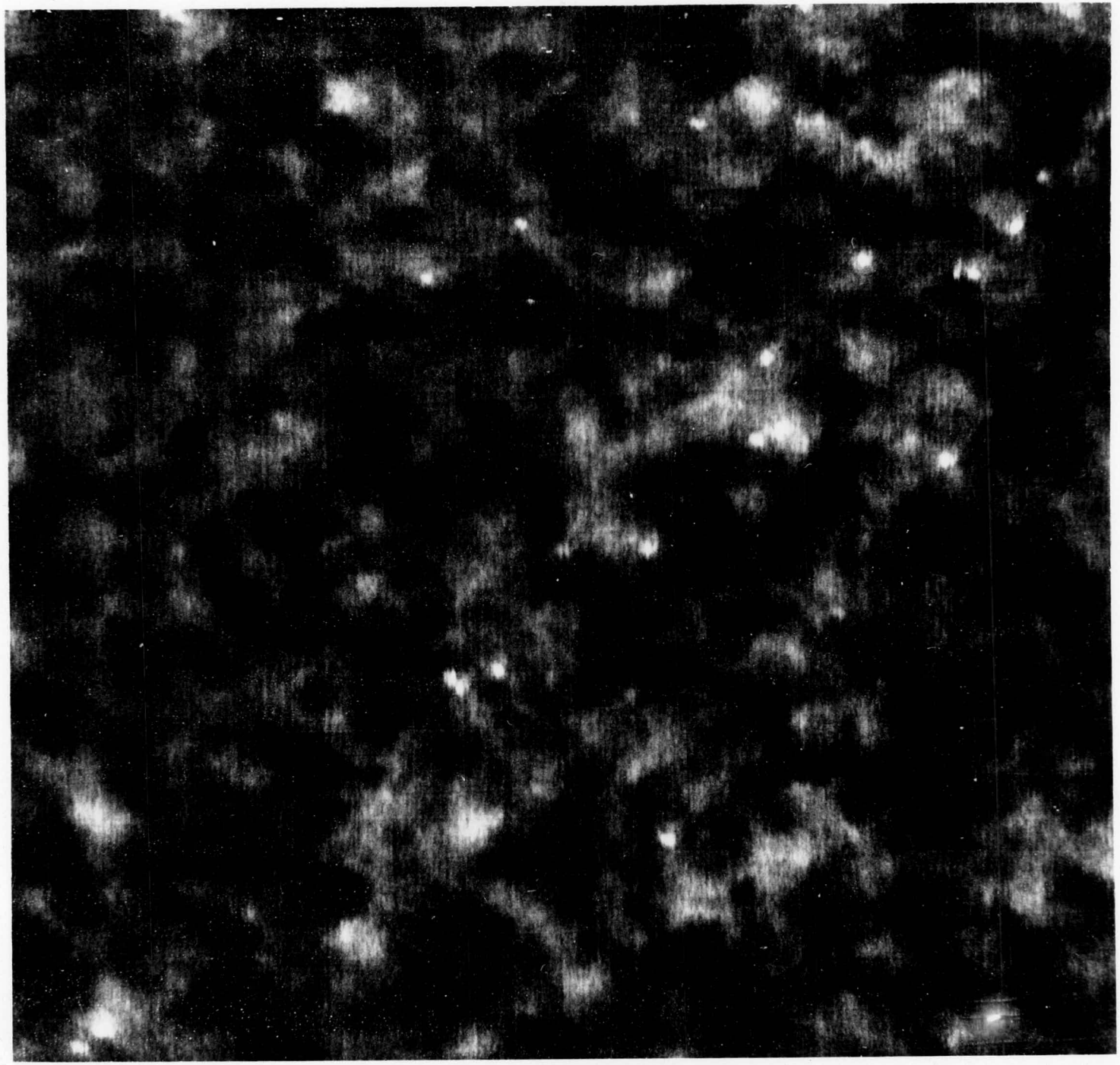

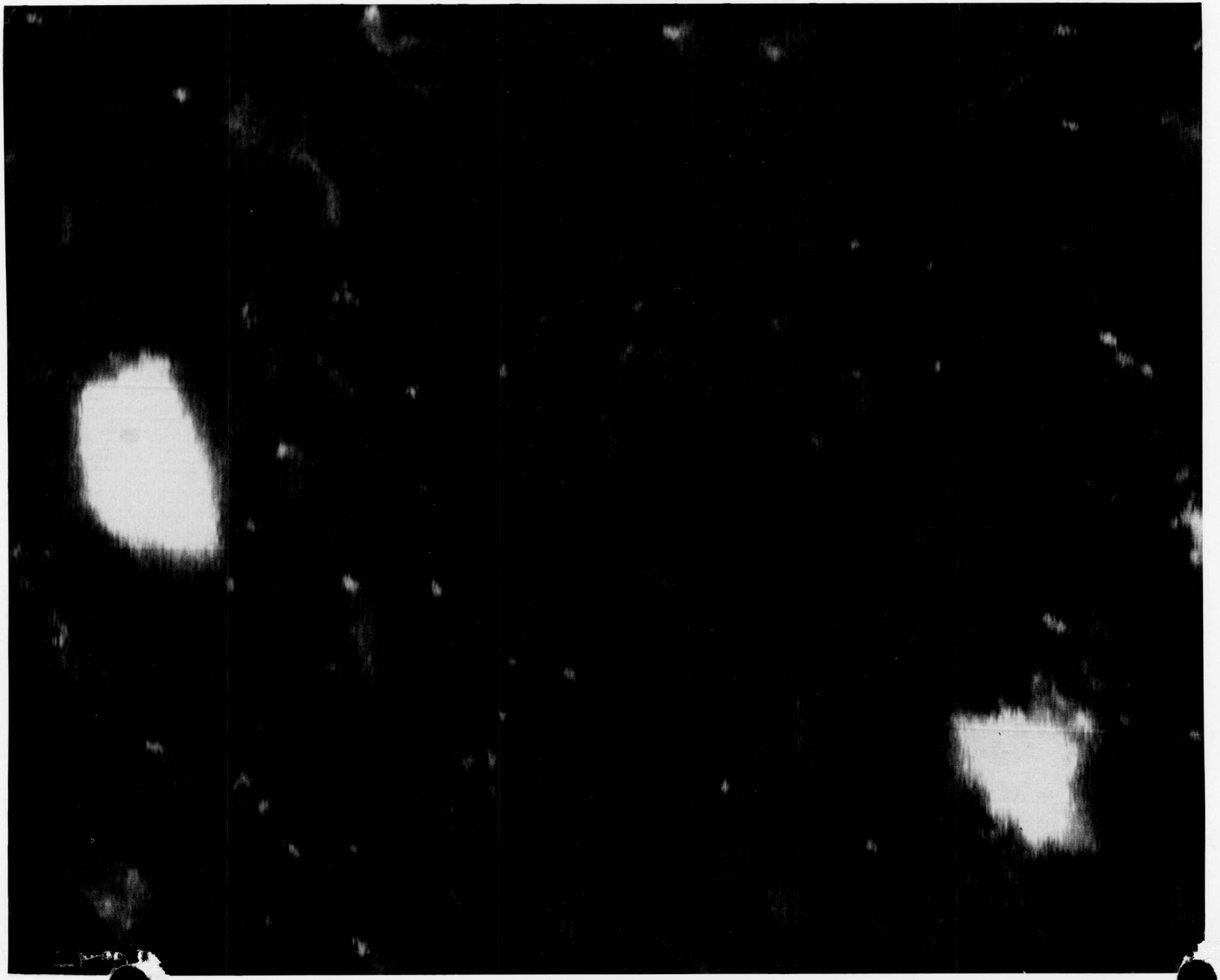

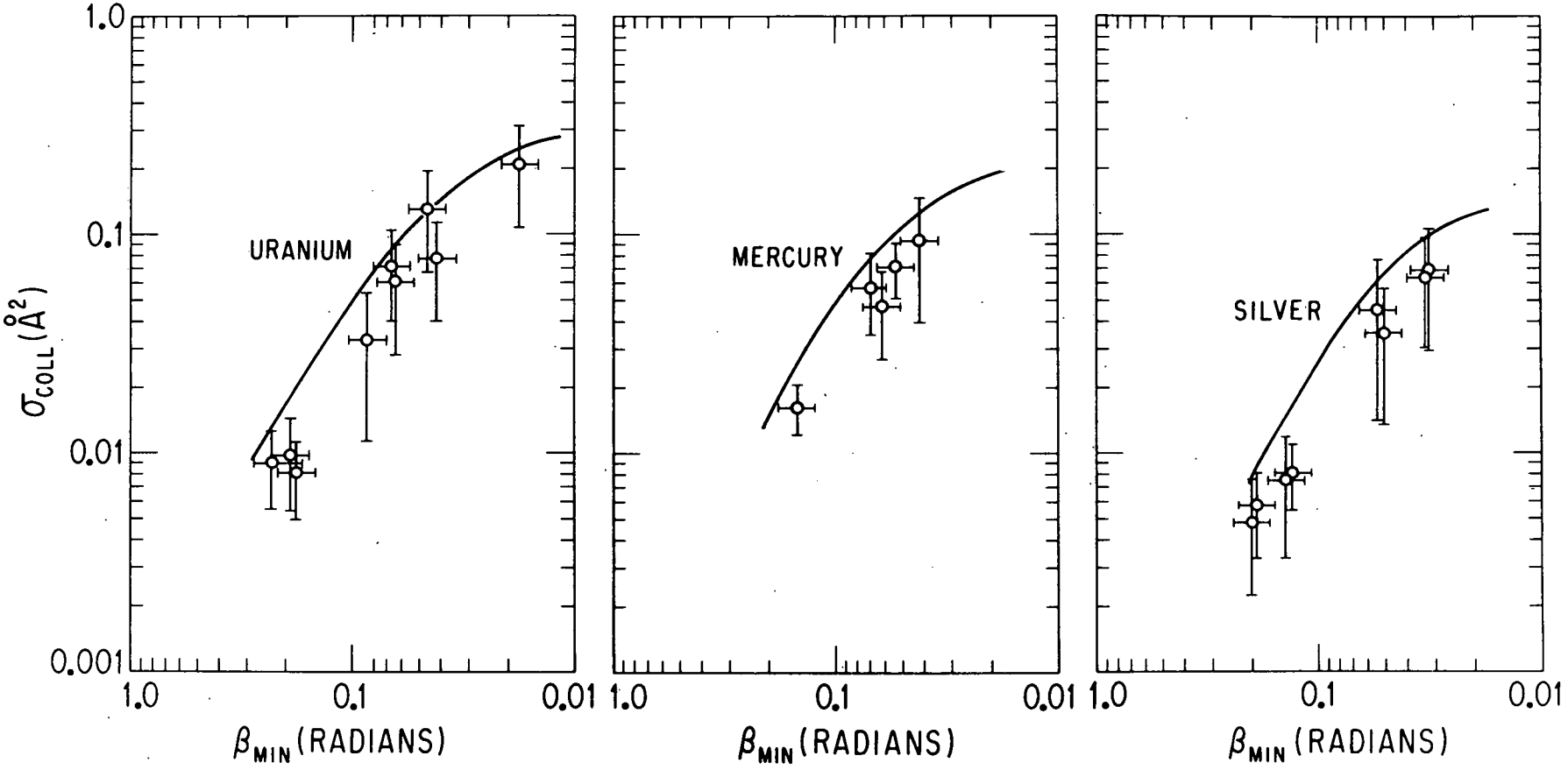
1.0
0.1
0.01
0.001
σ_{COLL} (Å^2)
URANIUM
MERCURY
SILVER
1.0
0.1
0.01
β_{MIN} (RADIANS)

Fig.8